Liu et al. *Zool. Res.* 2024, 45(5): 972−982
https://doi.org/10.24272/j.issn.2095-8137.2024.008
https://cstr.cn/32248.14.zr.2024.008

ZR | Zoological Research

Article Open Access

Anti-infective immune functions of type IV interferon in grass carp (*Ctenopharyngodon idella*): A novel antibacterial and antiviral interferon in lower vertebrates

Yuchen Liu[1,2], Wentao Zhu[1], Yanqi Zhang[1], Jingjing Zhang[1], Maolin Lv[1], Jianguo Su[1,2,*]

[1] *Hubei Hongshan Laboratory*, *College of Fisheries*, *Huazhong Agricultural University*, *Wuhan*, *Hubei* 430070, *China*

[2] *Laboratory for Marine Biology and Biotechnology*, *Qingdao Marine Science and Technology Center*, *Qingdao*, *Shandong* 266237, *China*

ABSTRACT

Type IV interferon (IFN-υ) is a recently discovered cytokine crucial for host defense against viral infections. However, the role and mechanisms of IFN-υ in bacterial infections remain unexplored. This study investigated the antibacterial and antiviral functions and mechanisms of grass carp (*Ctenopharyngodon idella*) IFN-υ (CiIFN-υ) both *in vivo* and *in vitro*. The CiIFN-υ gene was first identified and characterized in grass carp. Subsequently, the immune expression of CiIFN-υ significantly increased following bacterial challenge, indicating its response to bacterial infections. The eukaryotic recombinant expression plasmid of CiIFN-υ was then constructed and transfected into fathead minnow (FHM) cells. Supernatants were collected and incubated with four bacterial strains, followed by plate spreading and colony counting. Results indicated that CiIFN-υ exhibited more potent antibacterial activity against gram-negative bacteria compared to gram-positive bacteria and aggregated gram-negative bacteria but not gram-positive bacteria. *In vivo* experiments further confirmed the antibacterial function, showing high survival rates, low tissue edema and damage, reduced tissue bacterial load, and elevated proinflammatory response at the early stages of bacterial infection. In addition, the antiviral function of CiIFN-υ was confirmed through *in vitro* and *in vivo* experiments, including crystal violet staining, survival rates, tissue viral burden, and reverse transcription-quantitative real-time polymerase chain reaction (RT-qPCR). This study highlights the antibacterial function and preliminary mechanism of IFN-υ, demonstrating that IFN-υ possesses dual functions against bacterial and viral infections.

Keywords: Grass carp (*Ctenopharyngodon idella*); IFN-υ; Bactericidal activity; Antiviral activity; Antimicrobial immunity

INTRODUCTION

In 1957, Isaacs & Lindenmann (1957) identified a soluble antiviral substance in influenza virus studies, termed interferon (IFN). IFN is a type of glycoprotein known for its high biological activity, produced by recipient cells upon pathogen infection (Li et al., 2018) and playing a crucial role in the immune system and antiviral processes. Certain substances rely on IFN functions to exert their antiviral effects. For example, the hydroxy-coumarin drug C10 indirectly activates IFNs to clear spring viremia of carp virus (SVCV) in zebrafish (Liu et al., 2020). IFNs exhibit species-specific properties (Masters et al., 2010) and beyond their antiviral capabilities, act as antitumor and anti-epidemic agents (Baron et al., 1991).

IFNs induce an antiviral state in cells, effectively inhibiting a broad range of non-specific viruses (Isorce et al., 2016). Type I and III IFNs are known for their classical antiviral properties. Upon viral stimulation, the IFN signaling pathway is activated, enhancing the expression of various IFN-stimulated genes (ISGs) and the production of antiviral proteins (Lazear et al., 2019). These proteins disrupt various stages of the viral life cycle, preventing viral proliferation. Furthermore, IFNs orchestrate apoptosis and autophagy by modulating immune cell activities, thereby restricting tumor cell activities (Zhou et al., 2020). IFNs are classified into four types: I, II, III and IV (Chen et al., 2022; Su, 2022), three of which (types I, II, and IV) are present in teleosts. Type I IFNs are critical components of innate immunity and are the most widely studied (Stetson & Medzhitov, 2006). In mammals, IFN-γ is the sole type II isoform, whereas teleosts contain IFN-γ1 and IFN-γ2 (Igawa et al., 2006), with IFN-γ1 (also termed IFN-γ related (rel)) representing a fish-specific type II IFN. While type III IFNs in mammals, represented by IFN-λs, function similarly to type I IFNs by primarily contributing to antiviral defense (Lazear et al., 2019), these IFNs are lacking in teleosts. Type IV IFN (IFN-υ) was recently discovered, existing in cartilaginous fish to primitive mammals and differing from type I, II, and III IFNs

Received: 02 April 2024; Accepted: 07 May 2024; Online: 08 May 2024

Foundation items: This study was supported by the Biological Breeding-Major Projects (2023ZD04065)

*Corresponding author, E-mail: sujianguo@mail.hzau.edu.cn

in sequence characteristics, gene loci, phylogeny, and receptor complexes (Chen et al., 2022). Most vertebrate IFN-υ genes are located on unique and highly conserved loci, distinct from other IFN types, with phylogenetic analysis supporting IFN-υ as a monophyletic group (Chen et al., 2022, 2023b). IFNs can induce an antiviral state through ISGs, with the induction of ISGs and antiviral regulatory activity via IFN-υ *in vivo* verified in overexpressed, knockout, and knockdown zebrafish (Chen et al., 2022).

Grass carp (*Ctenopharyngodon idella*), a significant freshwater aquaculture species in China, encounters many stresses during cultivation, leading to frequent disease outbreaks and substantial economic losses. *Aeromonas hydrophila* and grass carp reovirus (GCRV) are particularly severe pathogens affecting grass carp culture. As multi-functional cytokines, IFNs present a novel approach to treating aquatic diseases due to their antiviral and immunomodulatory functions. IFNs have demonstrated potent efficacy in suppressing GCRV infections (Feng et al., 2014). Notably, the recently discovered IFN-υ also exhibits antiviral functions (Chen et al., 2022). We previously found that grass carp IFN1 (a type I IFN) demonstrates antibacterial activity both *in vitro* and *in vivo* (Xiao et al., 2021; Zhu et al., 2023). However, the biological functions and mechanisms of IFN-υ in bacterial infections remain unknown. In this study, we investigated the antibacterial and antiviral activities of CiIFN-υ both *in vitro* and *in vivo*. Results demonstrated that CiIFN-υ exhibited direct antibacterial activity *ex vivo*, induced an inflammatory response *in vivo*, reduced tissue damage, and enhanced antibacterial regulation. Furthermore, CiIFN-υ significantly increased survival rates, induced the expression of antiviral genes *Mx* and *viperin*, and suppressed viral load in tissues following GCRV infection in grass carp.

MATERIALS AND METHODS

Ethics statement

Grass carp (15±5 g) were acquired from the Chongqin An Ling Farm (China). All experiments were performed in accordance with the guidelines of the Laboratory Animal Center of Huazhong Agricultural University. All protocols were approved by the Ethics Committee on Animal Research at Huazhong Agricultural University (approval No.: HZAUFI-2023-0025). All efforts were made to minimize animal suffering.

Identification and cloning of CiIFN-υ

The IFN-υ protein sequence from zebrafish (*Danio rerio*) (Chen et al., 2022) was used as the query sequence to conduct a TBLASTN (https://blast.ncbi.nlm.nih.gov/) search of the most recent grass carp genome (HZGC01) (Wu et al., 2022) using TBtools (v.1.120) with an *E*-value cut-off of 1×10^{-5}. Gene exons were predicted using bioinformatics software (http://www.softberry.com/). The position of *IFN-υ* in the grass carp genome was determined by collinearity analysis. The full-length grass carp *IFN-υ* gene was amplified by polymerase chain reaction (PCR) and compared with that of zebrafish. Total RNA was extracted from the gill of grass carp following bacterial infection using TRIpure Reagent (Aidlab, China), according to manufacturer's instructions. RNA was then reverse-transcribed into cDNA using ABScript Neo RT Master Mix for quantitative real-time PCR (qPCR) with gDNA remover (ABclonal, China). Synthesized cDNA was stored at −20°C until use. The full-length sequence of *CiIFN-υ* was amplified using 2×Ftaq PCR MasterMix (ZOMANBIO, China). The gene encoding grass carp IFN-υ was identified and gene-specific primers are listed in Supplementary Table S1.

Protein structure prediction and charge analysis of CiIFN-υ

Three-dimensional (3D) model prediction for grass carp CiIFN-υ was conducted using the I-TASSER server (https://seq2fun.dcmb.med.umich.edu//I-TASSER/), which specializes in protein structure prediction. The resulting 3D model and net charge distribution were visualized utilizing PyMOL (v.2.5.4). Additionally, protein characterization was predicted using Expasy (https://web.expasy.org/protscale/).

Tissue distribution of CiIFN-υ in grass carp before and after bacterial infection

Healthy grass carp weighing approximately 15±5 g were housed in 300 L aquaria for a minimum of 2 weeks before the experiment. Tissue samples, including the brain, hepatopancreas, trunk kidney, blood, gill, hind intestine, spleen, skin, muscle, head kidney, heart, and eye, were collected from six healthy grass carp and preserved in TRIzol (Thermo Fisher, USA) for subsequent RNA extraction. The mRNA expression levels were analyzed using reverse transcription qPCR (RT-qPCR), with *18S rRNA* used as an endogenous reference (Su et al., 2011). The primers used for RT-qPCR analysis are detailed in Supplementary Table S1. Results were calculated using the $2^{-\Delta\Delta Ct}$ method.

Aeromonas hydrophila (ATCC 7966), isolated and maintained in our laboratory, was cultivated overnight in Luria Bertani (LB) medium and reinoculated at a ratio of 1:100 for 3 h on the day of the injection. Bacteria in the logarithmic growth phase were harvested, centrifuged at 12 000 r/min for 10 min at room temperature, and washed twice with phosphate-buffered saline (PBS). Subsequently, *A. hydrophila* was suspended in PBS, with 1×10^6 CFU of bacteria (100 μL) then intraperitoneally injected into the fish, while the control group received an equivalent volume of PBS. Following bacterial injection, samples were collected from six grass carp at four time points (0 h, 12 h, 24 h, and 48 h). Tissue samples from the head kidney, spleen, trunk kidney, and hepatopancreas were taken and stored in TRIzol reagent.

Expression of recombinant CiIFN-υ in fathead minnow (FHM) cell line

The complete coding sequence of CiIFN-υ was inserted into the pcDNA4-myc-His (pcDNA4) plasmid, which includes *Bam*H I and *Xho* I restriction enzyme sites. Subsequently, the recombinant plasmid pcDNA4-IFN-υ-myc-His was successfully generated using the EZNA Endo-Free Plasmid Mini Kit (Promega, USA), following the manufacturer's instructions. The ligated product, containing the original recombinant plasmid and desired fragment after enzymatic digestion, was transformed into DH5α cells. Three recombinant plasmids —pcDNA4-myc-His, pcDNA4-IFN-υ, and pcDNA4-IFN-υ-myc-His —were transfected into cells for 48 h, after which the supernatants were collected. The supernatant from the cells transfected with pcDNA4-IFN-υ contained the CiIFN-υ fusion protein, while the supernatant from the cells transfected with pcDNA4-myc-His was referred to as the pcDNA4 supernatant. Western blot analysis was performed to determine the concentration of the CiIFN-υ protein.

Verification of antibacterial activity of CiIFN-υ *in vitro*

The CiIFN-υ fusion protein obtained from the cell culture was filtered through a 0.22 μm membrane filter, and concentrated

using a 3 kDa ultrafiltration tube at 4 000 ×*g* for 20 min at 4°C. To reduce the salt content in the medium, a buffer solution (20 mmol/L Tris, pH 7.4) was added during the centrifugation processes. *Aeromonas hydrophila*, *Staphylococcus aureus* (ATCC 25923), *Escherichia coli* (ATCC 25922), and *Streptococcus agalactiae* (ATCC 13813) were cultured at their optimal temperatures for 12 h for revival, followed by an additional 3 h of growth (1:100). At the onset of the experiment, the bacterial suspension concentration was adjusted to an OD_{600} value of 0.5 using a spectrophotometer. Bacterial counts per unit volume were determined using a hemocytometer, resulting in approximately 1×10^8 CFU/mL. The bacterial concentration was further adjusted to 1×10^4 CFU/mL, and 5 μg of the target protein was dissolved in 100 μL of buffer solution. In the experimental group, the buffer solution containing dissolved CiIFN-υ was co-cultured with 100 μL of bacterial suspension at 37°C for 1 h (or 28°C for aquatic bacteria). An equal volume of supernatant from cells overexpressing the empty pcDNA4 vector was used as the control group and was also co-incubated with the bacterial suspension for the same duration. Following this, the protein and bacterial suspension mixture was spread onto LB agar plates and cultured for 12–16 h. Colony counts were independently conducted by two researchers. Each experiment was performed in triplicate.

A suspension of *E. coli*, *A. hydrophila*, *S. aureus*, and *S. agalactiae* at 1×10^8 CFU/mL was incubated with CiIFN-υ and an equal volume of supernatant overexpressing the empty pcDNA4 vector at room temperature for 1 h. Subsequently, 10 μL of 4',6-diamidino-2-phenylindole (DAPI, Beyotime, China) solution (10 μg/mL) was added to each mixture, followed by incubation at 25°C for 15 minutes. The resulting bacterial cell clusters were observed under a fluorescence microscope (Leica, Germany). All aggregation experiments were performed in triplicate.

Tissue bacterial load and histopathological changes in grass carp infected with *A. hydrophila*

Healthy grass carp were intraperitoneally injected with 1×10^6 CFU of *A. hydrophila* (100 μL). At 1 h after bacterial infection, the fish were divided into two groups: the experimental group received a 100 μL injection of CiIFN-υ (5 μg), while the control group received an equal volume of empty pcDNA4 supernatant. The fish were observed for pathological changes and survival over the subsequent 7 days. Spleen, head kidney, blood, and hind intestine samples were collected on days 1 (D1) and 3 (D3) post-treatment. These tissues were homogenized, diluted in sterile PBS, and cultured in Rimler-Shotts (RS) Agar medium. After 12 h of incubation at 28°C, *A. hydrophila* colonies on the plates were counted to quantify bacterial load in the tissues. On D3 post-treatment, the head kidney, trunk kidney, spleen, hind intestine, and gills were harvested and weighed for wet weight and dried weight (65°C for 5 days) to calculate the wet-to-dry weight ratio as an indicator of tissue edema. To better evaluate treatment effects, the head kidney, spleen, and hind intestine were also collected for histological examination by tissue sectioning. For the control group, FHM cell culture supernatant was harvested following overexpression of the empty pcDNA4 plasmid.

mRNA expression of immune-related genes after injection of *A. hydrophila*

Samples were collected on D1 and D3 post-infection. Grass carp were first anesthetized with 0.1% 3-aminobenzoic acid ethyl ester methanesulfonate (MS-222) (Sigma, China), followed by the collection of blood samples from the tail vein, and isolation of the hepatopancreas, spleen, hind intestine, and head kidney. Tissues were placed in 1.5 mL EP tubes containing 800 μL of TRIpure (Aidlab, China) and stored at −80°C for subsequent RNA extraction according to the manufacturer's instructions. Subsequently, Primer Premier v.5.0 was used to design gene-specific primers to detect the mRNA expression levels of *IL-1β* and *NF-κB1*.

Verification of antiviral activity of CiIFN-υ *in vitro* and *in vivo*

The recombinant plasmids pcDNA4-IFN-υ-myc (experimental group) and pcDNA4-myc-His (control group) were transfected into *C. idella* kidney (CIK) cells, initially obtained from the China Typical Culture Preservation Center (CCTCC), and subsequently cultured in our laboratory. RNA was extracted from the cells at different time points. The relative mRNA expression of the GCRV *vp56* gene was detected by RT-qPCR. The CIK cell line was cultured in DMEM supplemented with 10% fetal bovine serum (FBS, Gibco, USA), 100 U/mL penicillin (Sigma, USA), and 100 μg/mL streptomycin, in a carbon dioxide (5%) incubator at 28°C. Some cells were exposed to GCRV-II at various dilution ratios for crystal violet staining to observe pathological changes. For crystal violet staining, cells were first cultured in 24-well plates for 24 h, then challenged with GCRV for 48 h, chilled on ice, rinsed twice with pre-cooled PBS, and fixed with 4% methanol for 10 min. After removing the methanol, the cells were washed twice with PBS, stained with a 0.05% (w/v) crystal violet solution at room temperature for 30 min, then rinsed twice with distilled water and photographed. The GCRV infection protocol was as follows: Well-grown cells were transferred to culture plates and allowed to grow for 12–16 h to fully cover the culture substrate. The cells were then washed three times with pre-warmed (28°C) FBS-free fresh media to eliminate any FBS and antibiotic residue. Following this, 0.1–0.2 mL/cm^2 of pre-warmed (28°C) FBS-free fresh medium was added. GCRV was introduced to achieve an infection rate (MOI) of 0.1 and was diluted as needed prior to use.

Additionally, a grass carp model infected with GCRV-II was established. On D3 post-GCRV infection, the fish were segregated into two groups and injected with pcDNA4-IFN-υ or pcDNA4 supernatants, respectively. Tissue samples were collected on D5 and D7 post-injection to assess viral load and expression of antiviral genes *Mx2* and *viperin.*

Statistical analyses

Data are presented as mean±standard deviation (SD) at least three replicates. Significant differences were analyzed using Student's *t*-test for paired comparisons or one-way analysis of variance (ANOVA) for multiple comparisons. $P<0.05$ was considered a statistically significant difference (*: $P<0.05$; **: $P<0.01$; and ***: $P<0.001$).

RESULTS

Identification and sequence analysis of CiIFN-υ

Collinearity analysis revealed that the CiIFN-υ gene was located on chromosome 23 in the grass carp genome (Figure 1A). The preservation of homologous chromosomes was examined by comparing the genome region of zebrafish *IFN-υ* on chromosome 24 with that of grass carp *IFN-υ* on chromosome 23. The *CiIFN-υ* gene consisted of five exons

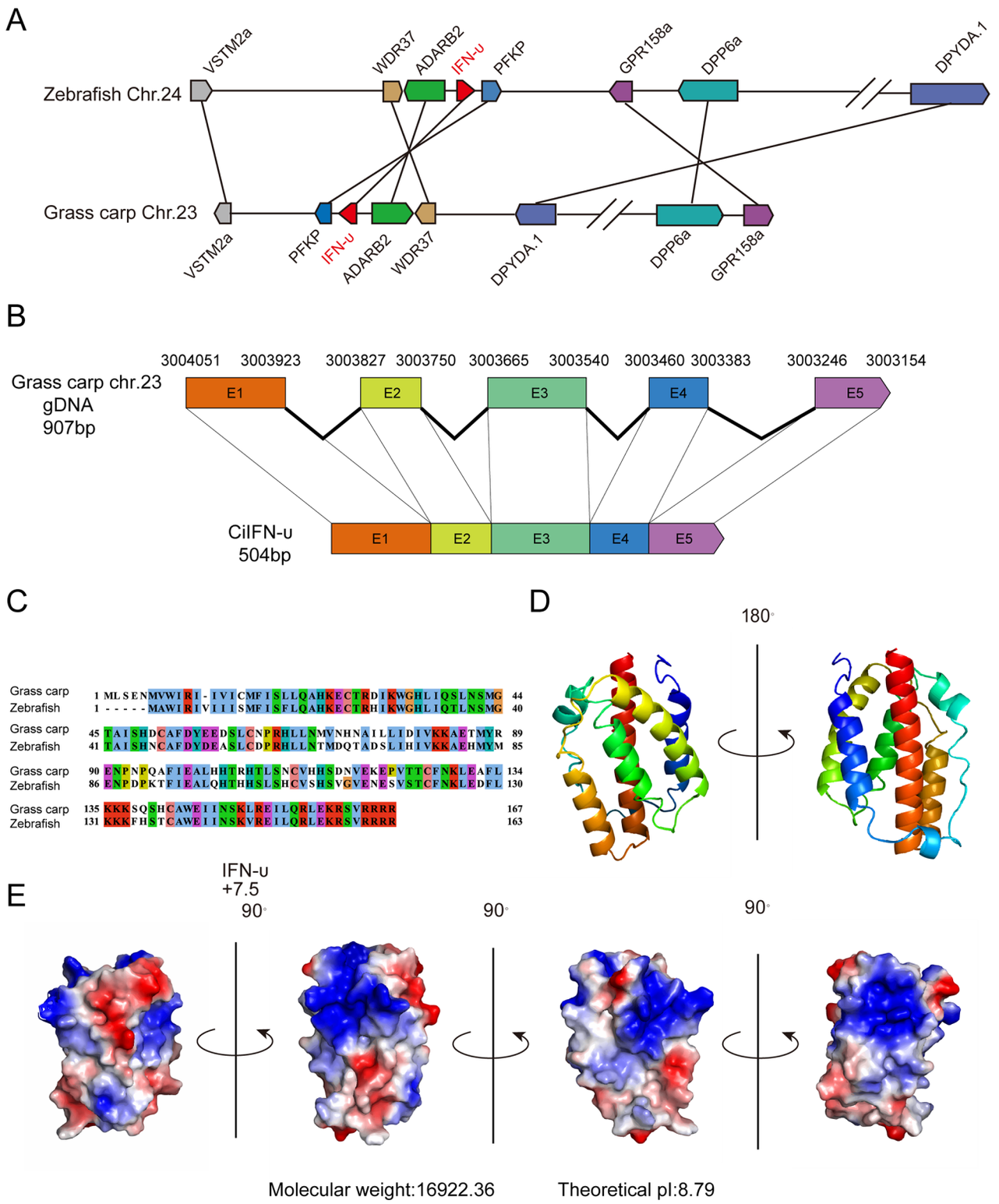

Figure 1 Collinearity analysis, gene structure, protein sequence alignment, three-dimensional (3D) structure, and charge prediction of CiIFN-u

A: Genome organization of genes surrounding *IFN-u* gene in zebrafish and grass carp, with gene orientations indicated by arrows. B: Gene structure of CiIFN-u, with exons shown as colored boxes and introns shown as black polylines. C: Comparison of protein sequences of CiIFN-u and zebrafish IFN-u (GenBank:MW547062) using Jalview software. D: 3D structure of CiIFN-u protein modeled by homology, based on CiIFN-u sequence excluding signal peptide. E: Electrostatic potential on the CiIFN-u protein surface, visualized using PyMOL. Positively charged regions are in blue, negatively charged regions are in red, and hydrophobic residues are in white.

(Figure 1B), with an open reading frame (ORF) spanning 504 nucleotides and encoding 167 amino acids. The gene sequence was deposited in NCBI (GenBank accession number OR916406). *IFN-u* was highly conserved between zebrafish and grass carp (Figure 1C). To elucidate the relationship of *IFN-u*, a phylogenetic tree of the four types of

IFNs in representative vertebrates was constructed, demonstrating the comparative homology of IFN-υ in different species and the homology of three types of IFNs in grass carp (Supplementary Figure S1). Furthermore, 3D structural prediction indicated that the α-helix was the dominant structure (Figure 1D). Analysis of CiIFN-υ using the ExPASy Compute pI/Mw tool demonstrated a molecular mass of 16.9 kDa and an isoelectric point at 8.72. The predicted surface potential suggested that CiIFN-υ had an overall positive charge of +7.5. (Figure 1E). These findings suggest that positively charged CiIFN-υ has the potential to resist bacteria.

CiIFN-υ is significantly induced after bacterial infection

Tissues were collected from healthy grass carp, and RT-qPCR revealed that *CiIFN-υ* was expressed in all 12 tested tissues, with higher expression in the gill and other immune-related tissues (Figure 2A). Subsequent bacterial infection experiments demonstrated that mRNA expression levels of *CiIFN-υ* increased at 12 h post-infection and then gradually returned to normal levels in the head kidney (Figure 2B), trunk kidney (Figure 2C), hepatopancreas (Figure 2D), and spleen (Figure 2E). These results suggest that *CiIFN-υ* rapidly responds to bacterial challenge.

CiIFN-υ demonstrates direct antibacterial effect *in vitro*

To determine the concentration of CiIFN-υ, western blot analysis was performed. The first five bands were created using a GST tag protein at increasing concentrations (0.005, 0.01, 0.02, 0.035, and 0.045 mg/mL), while the sixth band represented CiIFN-υ. The gray values of these six bands were measured, and a standard curve was constructed against the known concentrations to ascertain the concentration of CiIFN-υ, which was estimated to be approximately 10 μg/mL (Figure 3A). CiIFN-υ (5 μg) was incubated with a bacterial mixture (1×10^3 CFU) in a 200 μL volume and subsequently spread onto LB agar plates to determine colonies. Results showed that CiIFN-υ exhibited effective antibacterial activity against *S. aureus*, *A. hydrophila*, *S. agalactiae*, and *E. coli* (Figure 3B–D). Figure 3B presents only one set of images, with the corresponding parallel set of images provided in Supplementary Figure S2. Notably, CiIFN-υ possessed extensive antimicrobial capabilities, with more pronounced bactericidal effects on gram-negative bacteria than gram-positive bacteria. Moreover, when CiIFN-υ (same concentration) was co-cultured with the four distinct bacterial strains, followed by DAPI staining, the gram-negative bacteria demonstrated marked agglutination (Figure 3D). These results indicate that CiIFN-υ possesses direct antibacterial activity.

CiIFN-υ protects grass carp from *A. hydrophila* infection

Next, the therapeutic potential of CiIFN-υ was investigated *in vivo*. Grass carp were intraperitoneally injected with a lethal dose of *A. hydrophila* (1×10^6 CFU). At 1 h post-infection, the fish were administered CiIFN-υ (5 μg/fish), with pcDNA4 supernatant used as a control. The survival rates were monitored for one week, revealing that CiIFN-υ reduced mortality by 49% relative to the control group (Figure 4A). Tissue edema was assessed by comparing the wet/dry weight ratios of various tissues, including the head kidney, trunk

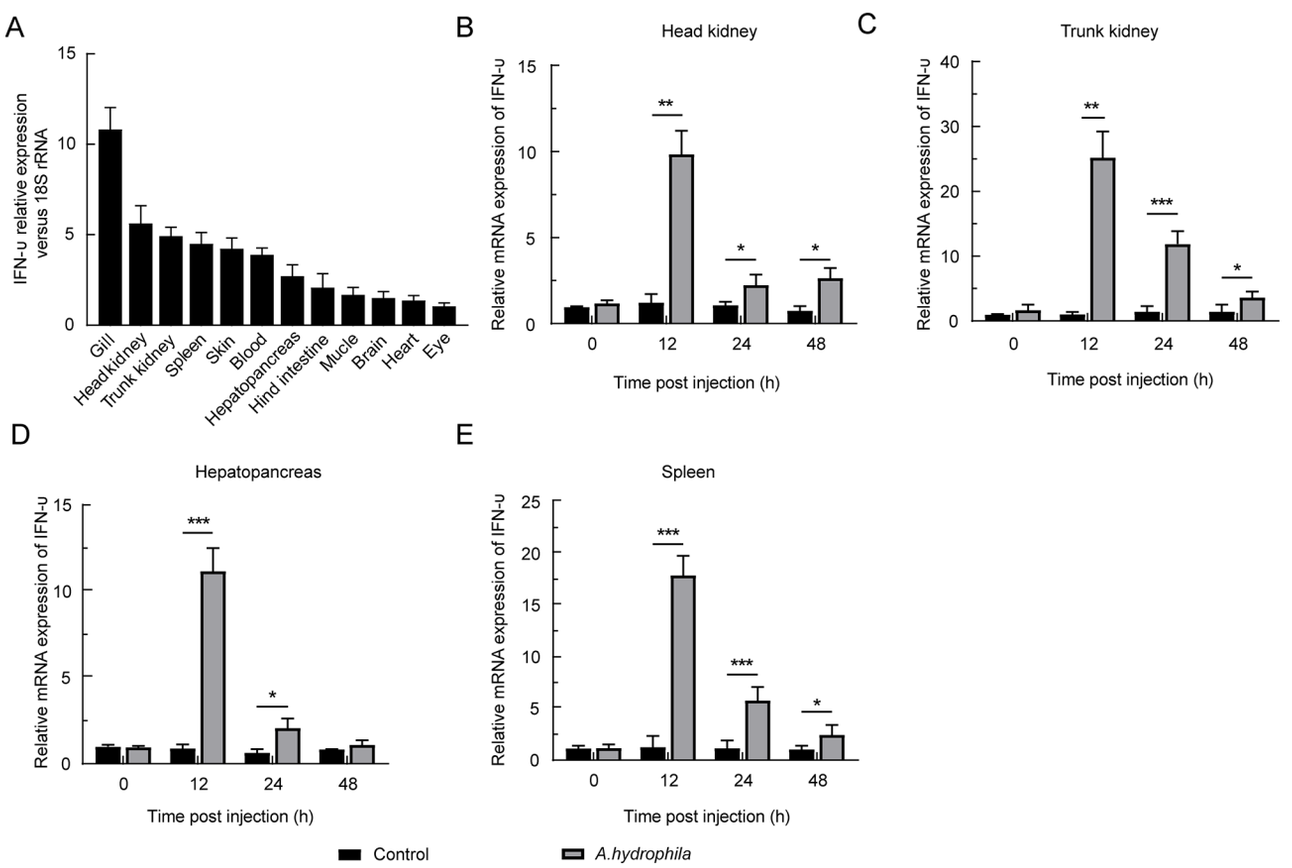

Figure 2 mRNA expression level of CiIFN-υ in grass carp

A: Tissue distribution of *CiIFN-υ* mRNA in healthy grass carp (n=6). B–E: Transcription levels of *IFN-υ* in head kidney, trunk kidney, hepatopancreas, and spleen of grass carp at 0 h, 12 h, 24 h, and 48 h post-bacterial infection. 18S rRNA was employed as the internal control. Experiments were conducted in triplicate, with results presented as mean±SD. ns: Not significant; *: P<0.05; **: P<0.01; ***: P<0.001.

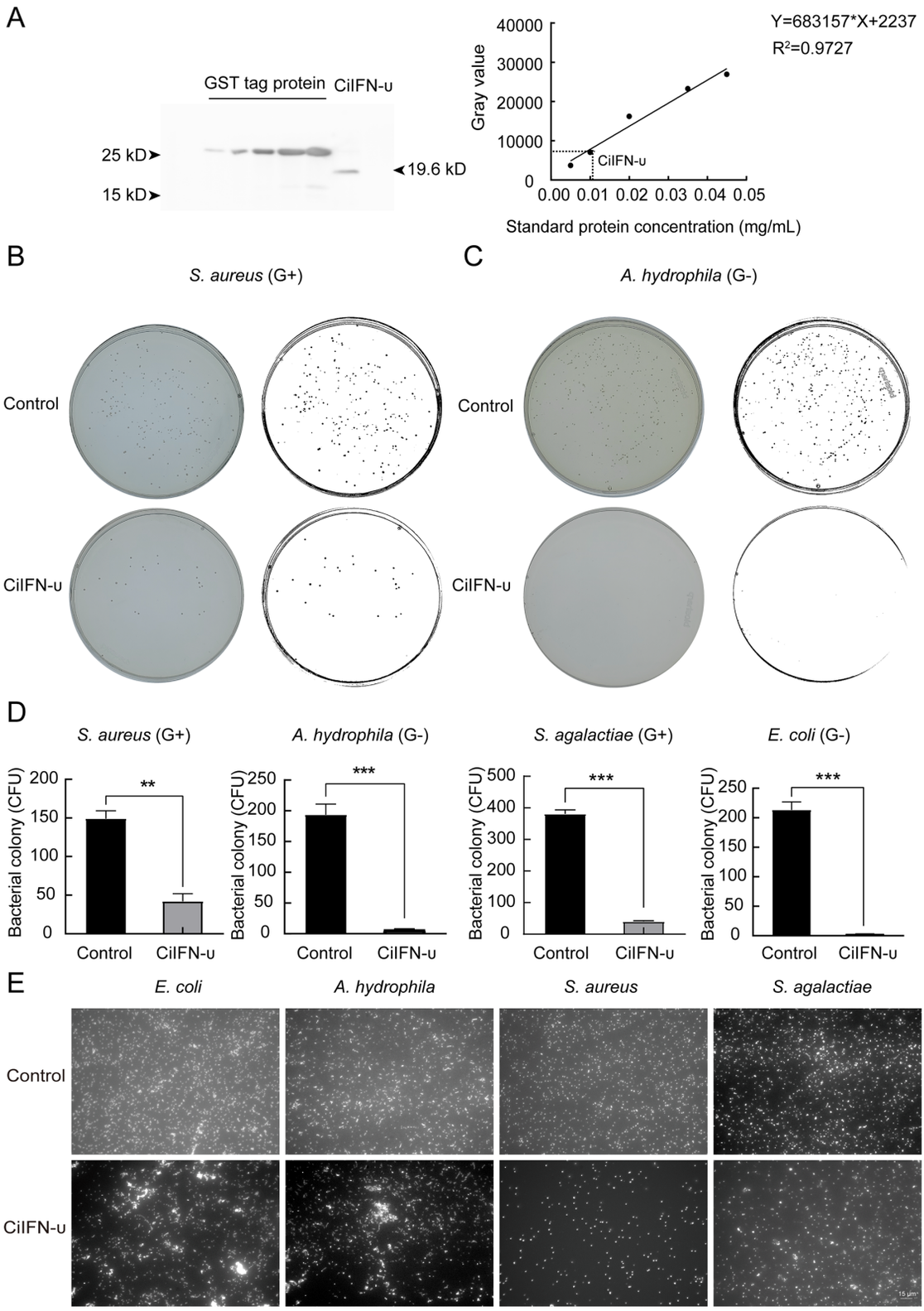

Figure 3 Evaluation of CiIFN-υ antibacterial activity *in vitro*

A: His-tagged CiIFN-υ detection by western blot analysis, with concentrations determined based on standard curve of gray values compared to known GST protein concentrations. CiIFN-υ was incubated with *S. aureus*, *A. hydrophila*, *S. agalactiae*, and *E. coli* to assess direct antibacterial effects. B: Inhibitory effects of CiIFN-υ against *S. aureus*. Images on the left represent original coated plates, images on the right represent enhanced visualization of original plates using ImageJ software. C: Inhibitory effects of CiIFN-υ against *A. hydrophila*. Images on the left represent original coated plates, images on the right represent enhanced visualization of original plates using ImageJ. D: Statistics of antibacterial effects of CiIFN-υ on four bacterial strains. E: CiIFN-υ was incubated with four bacterial strains, and bacterial aggregation was observed using a fluorescence microscope. Control: Supernatants were collected from FHM cells transfected with empty pcDNA4 vector. “G+” gram-positive bacteria, “G-” gram-negative bacteria. ns: Not significant; *: $P<0.05$; **: $P<0.01$; ***: $P<0.001$.

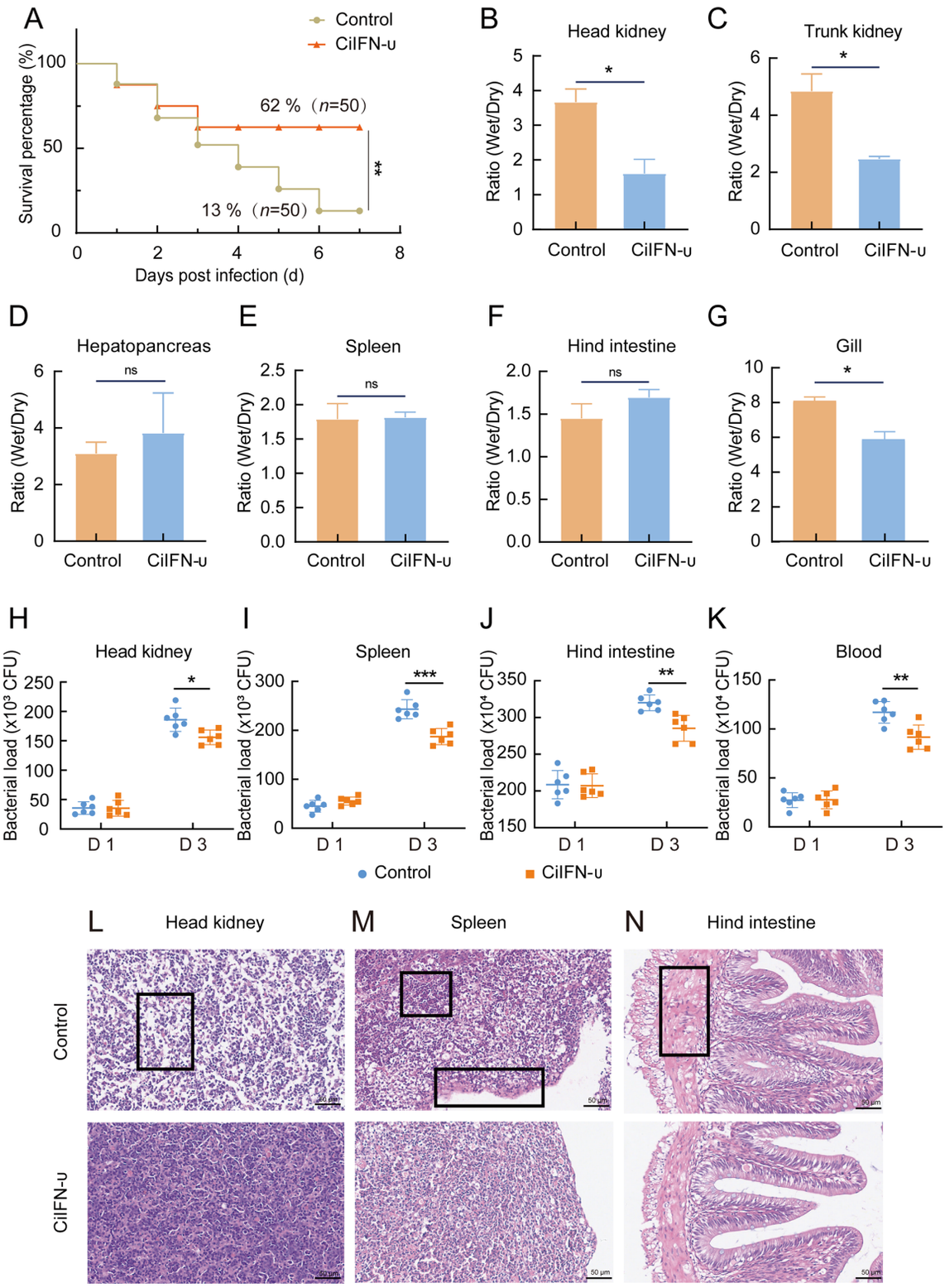

Figure 4 Therapeutic efficacy of CiIFN-u in grass carp following infection with *A. hydrophila*

Infective model of grass carp was established to determine the median lethal dose 50 (LD50) and assess the therapeutic effects of CiIFN-u (5 μg/fish). CiIFN-u was administered 1 h post-bacterial injection. A: Survival rates were recorded for one week following treatment (n=50 per group). B–G: Samples from various tissues, including head kidney, trunk kidney, hepatopancreas, spleen, hind intestine, and gill, were harvested on D3 post-treatment, and assessed for dry-to-wet weight ratios. H–K: Tissues, including head kidney, spleen, hind intestine, and blood, were sampled on D1 and D3 post-treatment (n=6). Collected samples were homogenized and diluted in sterile PBS and plated on selective medium, with colonies then counted after 12–16 h. L–N: Tissue sections were examined histopathologically, with images (left to right) showing sparse renal interstitial tissue in the head kidney, areas of nuclear consolidation and dissolved peritoneum in the spleen, and edema in the posterior intestinal wall. Control: Supernatants were collected from FHM cells transfected with empty pcDNA4 vector. Each experiment was conducted in triplicate, and results are presented as mean±SD. ns: Not significant; *: P<0.05; **: P<0.01; ***: P<0.001.

kidney, hepatopancreas, spleen, hind intestine, and gill (Figure 4B–G). CiIFN-υ notably decreased edema in the head kidney, trunk kidney, and gill. Furthermore, we quantified bacterial loads in the head kidney (Figure 4H), spleen (Figure 4I), hind intestine (Figure 4J), and blood (Figure 4K) on D1 and D3 post-infection. Results showed a significant reduction in bacterial load in the CiIFN-υ group on D3. Furthermore, histopathological examination was carried out using hematoxylin and eosin (H&E)-stained sections of the head kidney, spleen, and hind intestine from CiIFN-υ-treated fish. Results demonstrated denser cell populations in the head kidney (Figure 4L), reduced nuclear aggregation in the spleen, clearer peritoneal boundaries in the spleen (Figure 4M), thinner hind intestinal muscle layer, and diminished edema in the hind intestinal wall (Figure 4N) compared to the controls. Collectively, these findings suggest that CiIFN-υ exerts marked antibacterial activity against *A. hydrophila* infection *in vivo*.

CiIFN-υ promotes inflammatory response in *A. hydrophila*-infected grass carp

Aeromonas hydrophila infection results in severe bacterial septicemia in fish (Yang et al., 2016). Interleukin-1β (IL-1β), a pro-inflammatory cytokine, plays a pivotal role in regulating immune and inflammatory responses upon infection or immune challenge (Kitanaka et al., 2018). To elucidate the immune mechanisms of CiIFN-υ, the expression levels of *NF-κB1* and *IL-1β* were measured in the above therapeutic samples. Results showed that *NF-κB1* and *IL-1β* were significantly up-regulated in the head kidney, spleen, hind intestine, and blood on the first day following CiIFN-υ treatment (Figure 5), suggesting that CiIFN-υ induces a swift response to bacterial infection by enhancing pro-inflammatory factor production.

CiIFN-υ exhibits antiviral activity *in vitro* and *in vivo*

To determine the antiviral activity of CiIFN-υ *in vitro*, CIK cells were transfected with recombinant plasmid carrying the CiIFN-υ gene. Subsequently, these cells were challenged with different dilutions of GCRV-II, followed by crystal violet staining to observe cytological changes. A notable decrease in cytopathic effects was observed in cells treated with CiIFN-υ, indicating a cytoprotective function (Figure 6A). The mRNA expression levels of the *vp56* gene (GCRV) were then measured, with results showing a significant decrease in *vp56* expression in the CiIFN-υ-expressing cells compared to the control cells (Figure 6B). These findings suggest that CiIFN-υ exhibits antiviral activity *in vitro*.

Furthermore, the antiviral functions of CiIFN-υ were examined *in vivo*. A challenge assay was performed to examine the protective effects of CiIFN-υ against GCRV-II infection in grass carp. The mortality rates of infected grass carp were calculated for both the experimental group (CiIFN-υ) and control group (pcDNA4) over a period of seven days post-treatment (Figure 6C). Results indicated that CiIFN-υ treatment increased grass carp survival, enabling them to better withstand viral infection. Viral load in tissue samples was also measured based on the relative expression of *vp56*. Samples from the spleen, head kidney, and hind intestine were collected on D5 post-treatment. Treated tissues

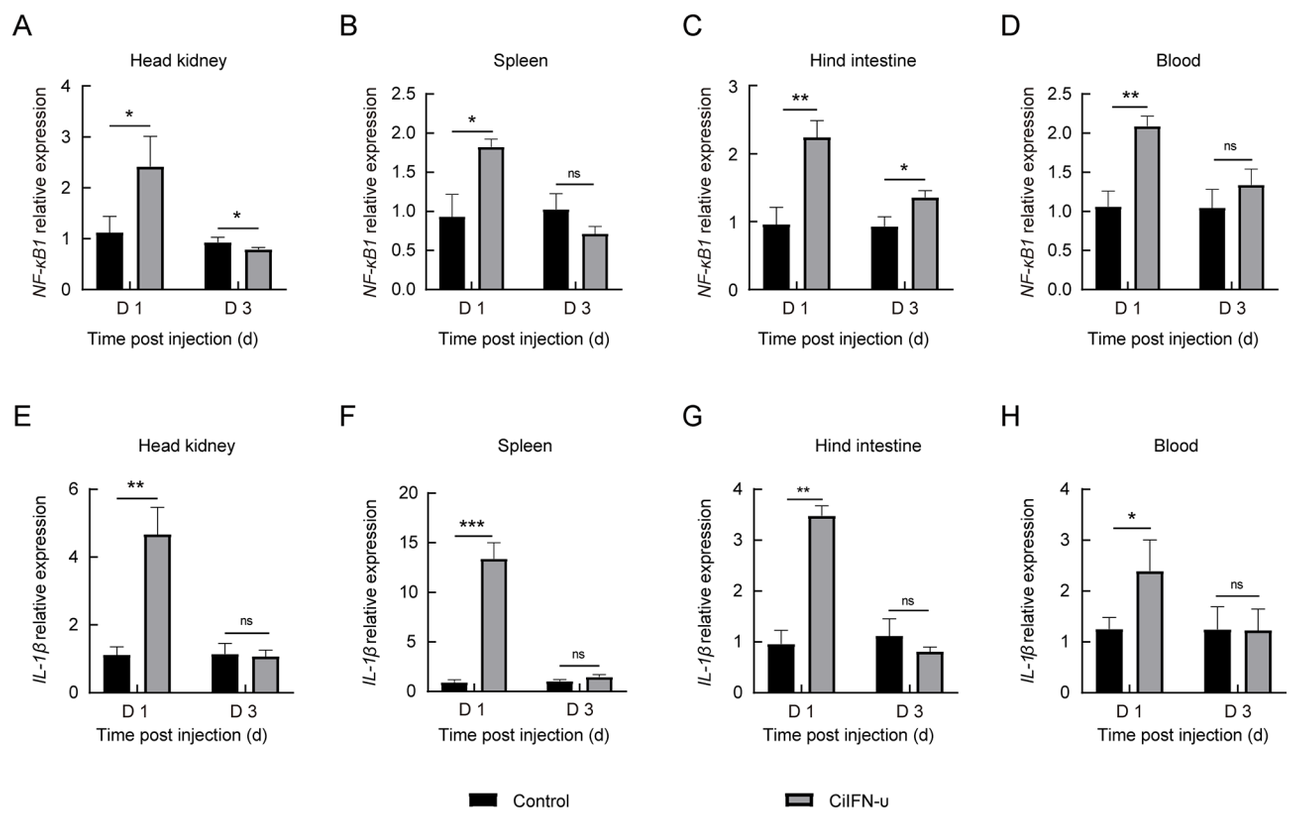

Figure 5 mRNA expression levels of representative immune factors in grass carp following *A. hydrophila* infection and CiIFN-υ injection

A–H: Expression levels of *NF-κB1* (A–D) and *IL-1β* (E–H) were assessed by RT-qPCR in the head kidney, spleen, hind intestine, and blood tissues of grass carp infected with *A. hydrophila* and treated with CiIFN-υ injection. *18S rRNA* gene was used as the internal reference. Control: Supernatants were collected from FHM cells transfected with empty pcDNA4 vector. Experiments were conducted in triplicate, and results were expressed as the mean ± SD. ns: Not significant; *: $P<0.05$; **: $P<0.01$; ***: $P<0.001$.

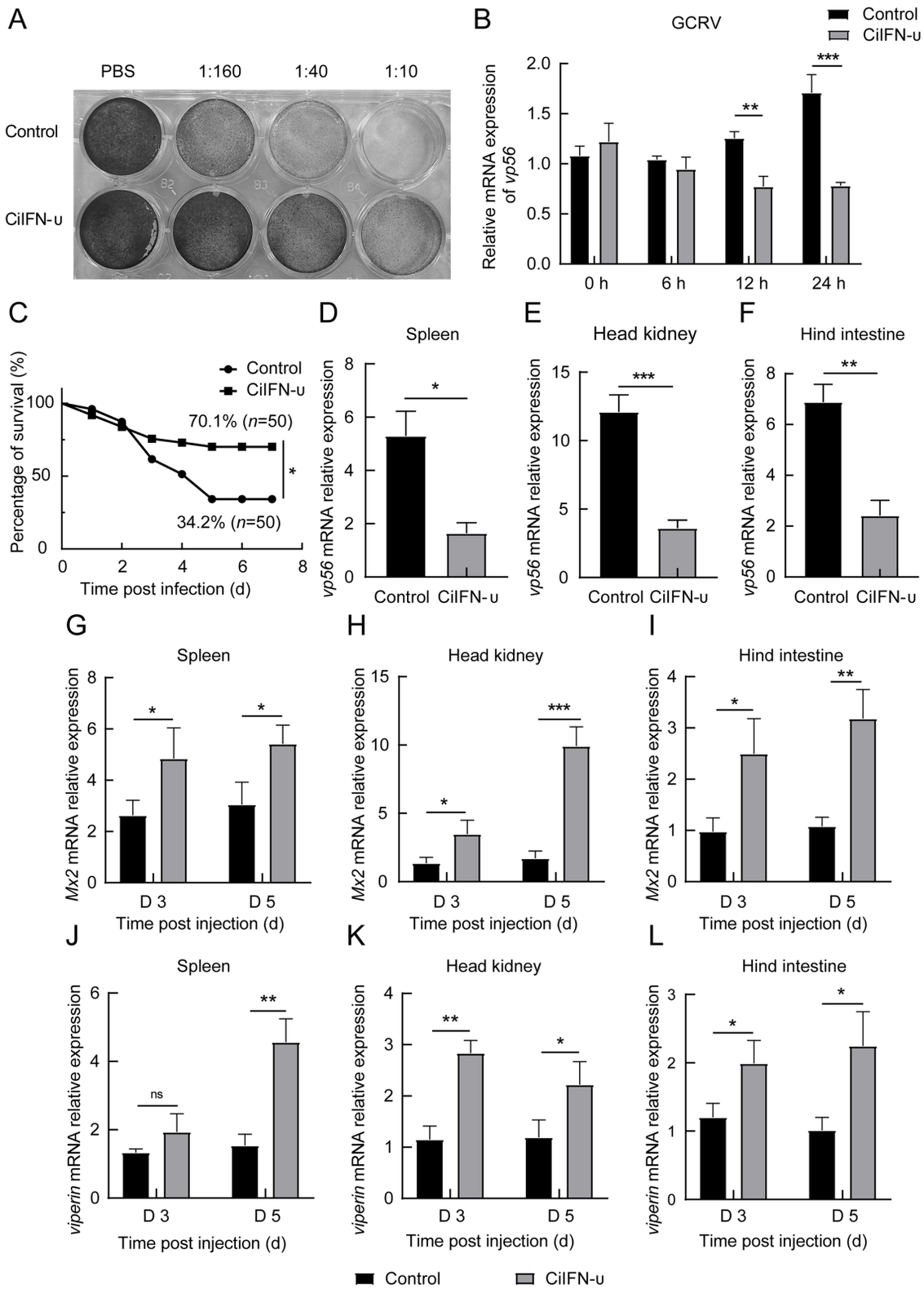

Figure 6 Detection of antiviral activity of CilFN-u

A: CIK cells transfected with pcDNA4-IFN-u were treated with different dilution ratios of GCRV-II and subjected to crystal violet staining to observe cytopathic effects. B: CIK cells in 6-well plates transfected with pcDNA4-IFN-u for 48 h were infected with GCRV, and samples were collected at different time points. Relative expression levels of *vp56* mRNA were measured by RT-qPCR with *EF1α* as the internal reference gene. CIK cells transfected with pcDNA4-myc-His served as the control. Grass carp reovirus (GCRV) infection model was established in grass carp, followed by treatment with CilFN-u injection (5 μg). C: Survival rates were calculated for one week (n=50 per group). D–F: Expression levels of *vp56* in the spleen, head kidney, and hind intestine were quantitatively assessed on D5. G–I: Expression level of *Mx2*. J–L: Expression of *Viperin* in the spleen, head kidney, and hind intestine was quantified on D3 and D5. Supernatant from FHM cells overexpressing pcDNA4 was utilized as the control. All experiments were conducted in triplicate, with outcomes expressed as mean±SD. ns: Not significant; *: P<0.05; **: P<0.01; ***: P<0.001.

exhibited a significant reduction in viral loads (Figure 6D–F). Additionally, the expression levels of two antiviral effector genes, *Mx2* (Figure 6G–I) and *viperin* (Figure 6J–L), were quantified on D3 and D5 post-treatment. Results showed that the antiviral genes in the CiIFN-υ-treated group were up-regulated from D3 post-treatment, with high expression maintained on D5. Collectively, these results confirm the antiviral activity of CiIFN-υ both *in vitro* and *in vivo*.

DISCUSSION

Type IV IFNs play a vital role in antiviral infections (Chen et al., 2022, 2023a). In the current study, we identified the IFN-υ gene in the grass carp genome, confirmed its antiviral functions both *in vitro* and *in vivo*, and explored its preliminary mechanisms. Notably, CiIFN-υ was found to induce antiviral effectors Mx2 and viperin. Mx2, belonging to the Mx family, is known for its powerful antiviral properties (Staeheli & Haller, 2018). Viperin, another antiviral protein, can be induced by various viruses, type I IFNs, poly (I:C), and lipopolysaccharide (Mattijssen & Pruijn, 2012). These antiviral effectors significantly suppressed GCRV-II viral loads in the head kidney, spleen, and hind intestine of grass carp, thereby enhancing survival rates.

Upon bacterial challenge, CiIFN-υ was significantly induced in the head kidney, trunk kidney, hepatopancreas, and spleen tissues of grass carp, suggesting a pivotal role in bacterial infections. NF-κB is known to promote the expression of inflammatory factors, while IL-1β is a key pro-inflammatory cytokine involved in defending against infections and injuries (Dinarello, 1996). Both NF-κB and IL-1β are critical in regulating the inflammatory response (Biswas et al., 2001; Lawrence, 2009). In the *A. hydrophila*-infected grass carp, the mRNA expression levels of *NF-κB1* and *IL-1β* were significantly up-regulated at an early stage after CiIFN-υ injection, indicating that CiIFN-υ enhances the inflammatory response. Following bacterial challenge, grass carp treated with CiIFN-υ showed increased survival rates (62% vs. 13%). We speculate that CiIFN-υ induces an inflammatory response by up-regulating inflammatory factors at an early stage of infection. Consequently, neutrophils, macrophages, and lymphocytes are attracted to the site of inflammation to combat and eradicate pathogens, thereby playing a protective role.

Many cytokines exhibit both antiviral and antibacterial activities. Interleukin-26 (IL-26), a proinflammatory cytokine, not only shows direct antimicrobial activity but also independently inhibits hepatitis C virus (HCV) replication (Beaumont et al., 2022), while grass carp IFN1 possesses both potent antiviral and antibacterial activity (Xiao et al., 2021; Zhu et al., 2023). In the present study, CiIFN-υ also demonstrated dual antiviral and antibacterial activity, especially against gram-negative bacteria. Interestingly, certain antimicrobial proteins and peptides can agglutinate bacteria due to nonspecific adhesion from hydrophobic interactions (Gorr et al., 2008). CiIFN-υ effectively agglutinated gram-negative bacteria but not gram-positive bacteria. Eosinophil cationic protein (ECP) is noted for its strong antimicrobial properties and specific agglutination of gram-negative bacteria at near-minimum inhibitory concentrations (Boix et al., 2008, 2012; Venge et al., 1999). The agglutination effect of CiIFN-υ parallels that of ECP, suggesting that the antibacterial mechanism of CiIFN-υ may partly involve bacterial agglutination.

In summary, type IV IFN displayed both antiviral and antibacterial activities. Notably, *CiIFN-υ*, located on chromosome 23, contained five exons and encoded a 167 amino acid protein with a net charge of +7.5. Following bacterial challenge, the mRNA expression level of *CiIFN-υ* was up-regulated. CiIFN-υ exhibited bactericidal activity *in vitro*, particularly against gram-negative bacteria, and induced agglutination of these bacteria. CiIFN-υ significantly improved survival rates against bacterial infection, reduced tissue edema, bacterial load, and damage, and enhanced inflammatory factors at the early stage of infection. Furthermore, CiIFN-υ exerted antiviral effects by promoting the expression of antiviral effectors and reducing viral gene expression. This dual anti-infective capacity greatly advances our understanding of IFN-υ functionality and highlights its potential in managing complex pathogenic challenges.

DATA AVAILABILITY

The grass carp IFN-υ sequence was uploaded to the National Center for Biotechnology Information (GenBank accession number: OR916406), China National Center for Bioinformation GenBase (C_AA070967.1), and Science Data Bank databases (DOI:10.57760/sciencedb.08195).

SUPPLEMENTARY DATA

Supplementary data to this article can be found online.

COMPETING INTERESTS

The authors declare that they have no competing interests.

AUTHORS' CONTRIBUTIONS

Y.L. and J.S. conceived the project and wrote the manuscript. Y.L. and W.Z. conducted the experiments and edited the manuscript. Y.Z. contributed to the analysis and constructive discussion. J.Z. and M.L. conducted the experiments. All authors read and approved the final version of the manuscript.

ACKNOWLEDGEMENTS

The authors would like to thank Dr. Changsong Wu, Dr. Xun Xiao, Dr. Bo Liang, Mr. Ning Xia, and Mr. Yuezong Xu for their technical advice and help with the experiments.

REFERENCES

Baron S, Tyring SK, Robert Fleischmann Jr W, et al. 1991. The interferons: mechanisms of action and clinical applications. *JAMA*, **266**(10): 1375–1383.

Beaumont É, Larochette V, Preisser L, et al. 2022. IL-26 inhibits hepatitis C virus replication in hepatocytes. *Journal of Hepatology*, **76**(4): 822–831.

Biswas DK, Dai SC, Cruz A, et al. 2001. The nuclear factor kappa B (NF-κB): a potential therapeutic target for estrogen receptor negative breast cancers. *Proceedings of the National Academy of Sciences of the United States of America*, **98**(18): 10386–10391.

Boix E, Salazar VA, Torrent M, et al. 2012. Structural determinants of the eosinophil cationic protein antimicrobial activity. *Biological Chemistry*, **393**(8): 801–815.

Boix E, Torrent M, Sánchez D, et al. 2008. The antipathogen activities of eosinophil cationic protein. *Current Pharmaceutical Biotechnology*, **9**(3): 141–152.

Chen L, Liu J, Yan J, et al. 2023a. Cloning and characterization of type IV interferon from black carp *Mylopharyngodon piceus*. *Developmental & Comparative Immunology*, **140**: 104614.

Chen SN, Gan Z, Hou J, et al. 2022. Identification and establishment of type IV interferon and the characterization of interferon-υ including its class II cytokine receptors IFN-υR1 and IL-10R2. *Nature Communications*, **13**(1): 999.

Chen SN, Li B, Gan Z, et al. 2023b. Transcriptional regulation and signaling of type IV IFN with identification of the ISG repertoire in an amphibian model. *Xenopus laevis. Journal of Immunology*, **210**(11): 1771–1789.

Dinarello CA. 1996. Biologic basis for interleukin-1 in disease. *Blood*, **87**(6): 2095–2147.

Feng XL, Su JG, Yang CR, et al. 2014. Molecular characterizations of grass carp (*Ctenopharyngodon idella*) TBK1 gene and its roles in regulating IFN-I pathway. *Developmental & Comparative Immunology*, **45**(2): 278–290.

Gorr SU, Sotsky JB, Shelar AP, et al. 2008. Design of bacteria-agglutinating peptides derived from parotid secretory protein, a member of the bactericidal/permeability increasing-like protein family. *Peptides*, **29**(12): 2118–2127.

Igawa D, Sakai M, Savan R. 2006. An unexpected discovery of two interferon gamma-like genes along with interleukin (IL)-22 and -26 from teleost: IL-22 and -26 genes have been described for the first time outside mammals. *Molecular Immunology*, **43**(7): 999–1009.

Isaacs A, Lindenmann J. 1957. Virus interference. I. The interferon. *Proceedings of the Royal Society Series B: Biological Sciences*, **147**(927): 258–267.

Isorce N, Testoni B, Locatelli M, et al. 2016. Antiviral activity of various interferons and pro-inflammatory cytokines in non-transformed cultured hepatocytes infected with hepatitis B virus. *Antiviral Research*, **130**: 36–45.

Kitanaka N, Nakano R, Kitanaka T, et al. 2018. NF-κB p65 and p105 implicate in interleukin 1β-mediated COX-2 expression in melanoma cells. *PLoS One*, **13**(12): e0208955.

Lawrence T. 2009. The nuclear factor NF-kappaB pathway in inflammation. *Cold Spring Harbor Perspectives in Biology*, **1**(6): a001651.

Lazear HM, Schoggins JW, Diamond MS. 2019. Shared and distinct functions of type I and type III interferons. *Immunity*, **50**(4): 907–923.

Li SF, Gong MJ, Zhao FR, et al. 2018. Type I interferons: distinct biological activities and current applications for viral infection. *Cellular Physiology and Biochemistry*, **51**(5): 2377–2396.

Liu L, Song DW, Liu GL, et al. 2020. Hydroxycoumarin efficiently inhibits spring viraemia of carp virus infection *in vitro* and *in vivo*. *Zoological Research*, **41**(4): 395−409.

Masters SL, Mielke LA, Cornish AL, et al. 2010. Regulation of interleukin-1β by interferon-γ is species specific, limited by suppressor of cytokine signalling 1 and influences interleukin-17 production. *EMBO Reports*, **11**(8): 640–646.

Mattijssen S, Pruijn GJM. 2012. Viperin, a key player in the antiviral response. *Microbes and Infection*, **14**(5): 419–426.

Staeheli P, Haller O. 2018. Human MX2/MxB: a potent interferon-induced postentry inhibitor of herpesviruses and HIV-1. *Journal of Virology*, **92**(24): e00709–18.

Stetson DB, Medzhitov R. 2006. Type I interferons in host defense. *Immunity*, **25**(3): 373–381.

Su JG. 2022. The discovery of type IV interferon system revolutionizes interferon family and opens up a new frontier in jawed vertebrate immune defense. *Science China Life Sciences*, **65**(11): 2335–2337.

Su JG, Zhang RF, Dong J, et al. 2011. Evaluation of internal control genes for qRT-PCR normalization in tissues and cell culture for antiviral studies of grass carp (*Ctenopharyngodon idella*). *Fish & Shellfish Immunology*, **30**(3): 830–835.

Venge P, Byström J, Carlson M, et al. 1999. Eosinophil cationic protein (ECP): molecular and biological properties and the use of ECP as a marker of eosinophil activation in disease. *Clinical & Experimental Allergy*, **29**(9): 1172–1186.

Wu CS, Ma ZY, Zheng GD, et al. 2022. Chromosome-level genome assembly of grass carp (*Ctenopharyngodon idella*) provides insights into its genome evolution. *BMC Genomics*, **23**(1): 271.

Xiao X, Zhu WT, Zhang YQ, et al. 2021. Broad-spectrum robust direct bactericidal activity of fish IFNφ1 reveals an antimicrobial peptide-like function for type I IFNs in vertebrates. *The Journal of Immunology*, **206**(6): 1337–1347.

Yang Y, Yu H, Li H, et al. 2016. Transcriptome profiling of grass carp (*Ctenopharyngodon idellus*) infected with *Aeromonas hydrophila*. *Fish & Shellfish Immunology*, **51**: 329−336.

Zhou LL, Zhang YQ, Wang YQ, et al. 2020. A dual role of Type I interferons in antitumor immunity. *Advanced Biosystems*, **4**(11): 1900237.

Zhu WT, Zhang YQ, Liao ZW, et al. 2023. IFN1 enhances thrombocyte phagocytosis through IFN receptor complex-JAK/STAT-complement C3.3-CR1 pathway and facilitates antibacterial immune regulation in teleost. *The Journal of Immunology*, **210**(8): 1043–1058.